JBIC Journal of Biological Inorganic Chemistry
https://doi.org/10.1007/s00775-019-01711-z

ORIGINAL PAPER

Metal coordination and peripheral substitution modulate the activity of cyclic tetrapyrroles on αS aggregation: a structural and cell-based study

Nazareno González[1] · Iñaki Gentile[1] · Hugo A. Garro[1,2] · Susana Delgado-Ocaña[1] · Carla F. Ramunno[1] · Fiamma A. Buratti[1] · Christian Griesinger[3] · Claudio O. Fernández[1,3]

Received: 18 June 2019 / Accepted: 28 July 2019

Abstract

The discovery of aggregation inhibitors and the elucidation of their mechanism of action are key in the quest to mitigate the toxic consequences of amyloid formation. We have previously characterized the antiamyloidogenic mechanism of action of sodium phtalocyanine tetrasulfonate ([$Na_4(H_2PcTS)$]) on α-Synuclein (αS), demonstrating that specific aromatic interactions are fundamental for the inhibition of amyloid assembly. Here we studied the influence that metal preferential affinity and peripheral substituents may have on the activity of tetrapyrrolic compounds on αS aggregation. For the first time, our laboratory has extended the studies in the field of the bioinorganic chemistry and biophysics to cellular biology, using a well-established cell-based model to study αS aggregation. The interaction scenario described in our work revealed that both N- and C-terminal regions of αS represent binding interfaces for the studied compounds, a behavior that is mainly driven by the presence of negatively or positively charged substituents located at the periphery of the macrocycle. Binding modes of the tetrapyrrole ligands to αS are determined by the planarity and hydrophobicity of the aromatic ring system in the tetrapyrrolic molecule and/or the preferential affinity of the metal ion conjugated at the center of the macrocyclic ring. The different capability of phthalocyanines and meso-tetra (*N*-methyl-4-pyridyl) porphine tetrachloride ([$H_2PrTPCl_4$]) to modulate αS aggregation in vitro was reproduced in cell-based models of αS aggregation, demonstrating unequivocally that the modulation exerted by these compounds on amyloid assembly is a direct consequence of their interaction with the target protein.

Keywords Misfolding · Amyloid · Neurodegeneration · Inhibitors

Introduction

Parkinson's disease (PD) is the second most common age-related neurodegenerative disorder after Alzheimer's disease, affecting millions of people worldwide [1]. Most of the PD patients receive their diagnosis at the age of 50–60, with clinical symptoms comprising motor impairments including bradykinesia, tremor, akinesia, rigidity and other non-motor symptoms [2]. The motor manifestations are attributed to the irreversible loss of dopaminergic neurons of the *substantia nigra* (*SN*) *pars compacta*, whereas the formation of proteinaceous inclusions known as Lewy bodies is recognized as the pathological hallmark of the disease [3]. Two decades ago, immunostaining of SN sections of PD patients indicated that the protein α-synuclein (αS) is the major component of Lewy bodies, suggesting a role of αS in this pathology [4–6]. Lewy bodies are not restricted to PD but also found in other neurodegenerative diseases such

Nazareno Gonzalez and Iñaki Gentile contributed equally to the manuscript.

Electronic supplementary material The online version of this article (https://doi.org/10.1007/s00775-019-01711-z) contains supplementary material, which is available to authorized users.

✉ Claudio O. Fernández
fernandez@iidefar-conicet.gob.ar; cfernan@gwdg.de

[1] Max Planck Laboratory for Structural Biology, Chemistry and Molecular Biophysics of Rosario (MPLbioR, UNR-MPIbpC) and Instituto de Investigaciones para el Descubrimiento de Fármacos de Rosario (IIDEFAR, UNR-CONICET), Universidad Nacional de Rosario, Ocampo y Esmeralda, S2002LRK Rosario, Argentina

[2] Facultad de Química, Bioquímica y Farmacia, Universidad Nacional de San Luis, Chacabuco y Pedernera, CP 5700, San Luis, Argentina

[3] Department of NMR-based Structural Biology, Max Planck Institute for Biophysical Chemistry, Am Fassberg 11, 37077 Göttingen, Germany

Published online: 05 September 2019

multiple system atrophy and dementia with Lewy bodies, collectively known as synucleinopathies [7–9]. Accordingly, over the last 20 years effort of numerous laboratories led to the development of different in vitro and in vivo systems, which were targeted to characterize αS, its aggregation, and the formation of Lewy bodies to shed light on the mechanism of pathogenesis in PD [10–19].

α-Synuclein (14 kDa) is a highly soluble, intrinsically disordered protein that is abundantly expressed in the brain and predominantly localizes to presynaptic terminals, in close proximity to synaptic vesicles [20–24]. Structurally, monomeric αS is characterized by an amphipathic N-terminal region (residues 1–60), involved in lipid binding; a central, highly hydrophobic self-aggregating sequence known as non-amyloid β component (NAC; residues 61–95), presumed to initiate fibrillation; and the acidic C-terminal region (residues 96–140), that is critical for blocking rapid αS filament formation [25–28] (Fig. 1a). Since misfolding and amyloid aggregation of αS is thought to play a critical role in PD [29], the aggregation pathway of the protein represents then an obvious target for therapeutic intervention in this disorder [16–19, 30, 31]. Therefore, understanding the mechanistic basis behind αS amyloid assembly and its inhibition is of high clinical importance. In this context, the discovery of small molecules targeting disease-associated protein aggregation is considered one of the most active therapeutic approaches toward neurodegenerative disorders [17, 19, 32]. Not only small molecules have been shown to modulate the aggregation of amyloid proteins both in vitro and in vivo, but have been also used as molecular and structural probes to gain insight into the amyloid aggregation process [33–36]. From the screening of large libraries of small molecules, potential candidates with different chemical structures were found to modulate the aggregation of distinct amyloid proteins [17, 37–55]. Notably, poly-aromatic scaffolds belonging to flavonoids, polyphenols, porphyrins, and phthalocyanines were predominantly identified by these screenings. Indeed, distinct variants of phthalocyanines and porphyrins have been tested for their ability to impair amyloid assembly of proteins linked to neurodegeneration [36, 37, 56–59]. These molecules are cyclic tetrapyrroles, a class of compounds whose distinguished characteristic is the planarity and hydrophobicity of its aromatic ring system. The phtalocyanine tetrasulfonate (PcTS) compounds are among the most widely investigated tetrapyrroles [56]. The structure of PcTS contains four sulfonic acid groups at the periphery of the aromatic rings, whereas the central cavity of the molecule can remain ligand-free or conjugated to metal ions of various valences (Fig. 1b).

Particularly, [$Na_4(H_2PcTS)$] was shown to exhibit anti-scrapie activity [41, 43, 60–62] and inhibition of αS [35, 37, 57] and tau amyloid assembly [58]. However, this compound was not able to impair the amyloid fibril formation of Aβ40 [36]. These results argued against the hypothesis that cyclic tetrapyrroles might have a common mechanism of action in slowing the formation of a variety of pathological aggregates. From a mechanistic perspective, and to fully understand the way these compounds might modulate protein aggregation, it is not only of paramount importance to decipher the structural basis of the implied protein-ligand interactions but also to investigate the molecular requirements of the small molecules that are critical for efficient and specific anti-amyloid activity. In that direction, in this work we studied how the nature of the conjugated metal ion and peripheral substituents in tetrapyrrolic compounds may influence or modulate the activity of these compounds on the amyloid fibril assembly of the protein αS. Our results demonstrated that both the nature of the metal ions conjugated to the central nitrogens and the properties of the functional groups at the periphery of the aromatic macrocycle

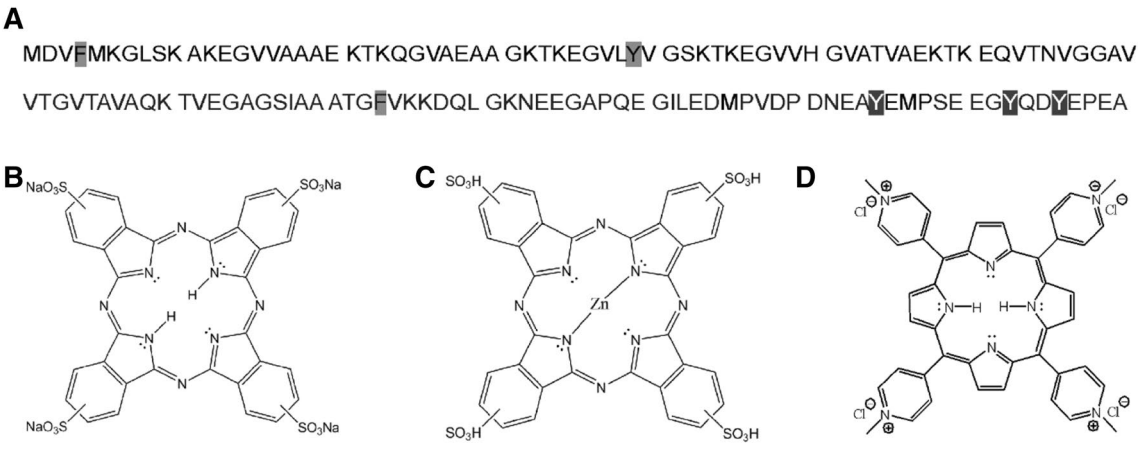

Fig. 1 **a** Primary sequence of the full-length protein αS. Aromatic residues are shaded in gray at the N-terminal and NAC regions, and in black at the C terminus. Chemical structure of phthalocyanine and porphine compounds: **b** [$Na_4(H_2PcTS)$], **c** [$Zn(H_4PcTS)$] and **d** [$H_2PrTPCl_4$]

in phthalocyanines and porphyrins are factors that influence the location of these compounds at well-defined regions of αS and its interaction with specific residues in the protein sequence. Interestingly, we found that the interaction profile of these molecules with αS correlates directly with their modulatory (inhibition/acceleration) effects on the amyold fibril assembly of the protein. Most importantly, the effects observed in vitro were reproduced on a well-established cell-based model for the study of αS aggregation. Overall, the results reported in this work provide a framework in which bioinorganic chemistry, biophysics and cell biology can be combined to understand the structural rules directing the interaction of aggregation inhibitors with target proteins and their implications on its amyloid fibril assembly.

Materials and methods

Protein and reagents

Unlabeled and ^{15}N isotopically enriched N-terminally acetylated αS was obtained by co-transforming *E. coli* BL21 with the plasmid harboring the wild type αS gene and a second one that encodes for the components of yeast NatB acetylase complex [63]. Both plasmids carried different antibiotic resistance, namely Ampicillin and Chloramphenicol to select the doubly transformed *E. coli* colonies. Purification was carried out as previously reported [64] with the exception that both antibiotics were included in the growth flasks to avoid plasmid purge during growth and expression. The final purity of the αS samples was determined by SDS-PAGE. Purified protein samples were dissolved in 20 mM MES buffer supplemented with 100 mM NaCl at pH 6.5 (Buffer A). Protein concentrations were determined spectrophotometrically by measuring absorption at 274 nm and using an epsilon value of 5600 M^{-1} cm^{-1}. Sodium phtalocyanine tetrasulfonate ([$Na_4(H_2PcTS)$]) was purchased from MP Biomedicals (Solon, Ohio); aluminium phthalocyanine chloride tetrasulfonic acid ([$Al(H_4PcTS)Cl$]), zinc phthalocyanine tetrasulfonic acid ([$Zn(H_4PcTS)$]) and *meso-tetra* (*N-methyl-4-pyridyl*) *porphine tetrachloride* ([$H_2PrTPCl_4$]) were from Frontier Scientific Inc. (Logan, Utah).

NMR experiments

NMR spectra were registered on a Bruker 600 MHz HD Avance III spectrometer, equipped with a cryogenically cooled triple resonance ^{1}H ($^{13}C/^{15}N$) TCI probe. Two-dimensional 2D ^{1}H–^{15}N heteronuclear single quantum correlation (HSQC) experiments were performed with pulsed-field gradient enhanced pulse sequences [65] on 50–100 μM ^{15}N-labeled protein samples dissolved in buffer A, at 15 °C. One-dimensional 1D ^{1}H-NMR experiments were acquired at 15 °C on 50–100 μM unlabeled αS samples dissolved in buffer A. Aggregation did not occur under these low-temperature conditions and absence of stirring. For the mapping experiments, ^{1}H–^{15}N HSQC amide cross-peaks affected during titrations with the ligand molecules were identified by comparing their intensities (I) with those of the same cross-peaks in the data set of free protein (I_0) [35]. The I/I_0 ratios of 90–100 non-overlapping cross-peaks were plotted as a function of the protein sequence to obtain the intensity profiles. Acquisition and processing of NMR spectra were performed using TOPSPIN 7.0 (Bruker Biospin). 2D spectra analysis and visualization were performed with CCPN.

Electron microscopy

10-μl aliquots withdrawn from aggregation reactions of αS in the absence or presence of phthalocyanines molecules and [$H_2PrTPCl_4$] were adsorbed onto Formvar/carbon-coated copper grids (Pella Inc.) and negative stained with 2% (w/v) uranyl acetate. Images were obtained at various magnifications (1000–90,000×) using a Philips CM120 transmission electron microscope, at the Facility for Transmission Electron Microscopy of the Max Planck Institute for Biophysical Chemistry (Göttigen).

Cell culture and transfection

For the studies with cell-based models of αS aggregation, H4 neuroglioma cells (ATCC® HTB-148™) were maintained at 5% CO_2 and 37 °C in Dulbecco's Modified Eagle's Medium (DMEM) (Gibco) supplemented with 10% fetal bovine serum (Gibco) and 1% Penicillin Streptomycin (Gibco). 1 day before transfection cells were seeded in 12-well plates. Cells were co-transfected with plasmids encoding a C-terminally modified αS (SynT construct) and synphilin-1 [15] using FuGene (Promega), according to the manufacturer's instructions. After 24 h of transfection, phthalocyanines and [$H_2PrTPCl_4$] were added to the cells in concentrations of 10 μM. Cells were treated with buffer A to exclude vehicle effects. Inclusion formation was assessed 48 h post-transfection.

Immunocytochemistry

Cells were fixed with 4% paraformaldehyde in PBS 48 h after transfection and start of phthalocyanines and [$H_2PrTPCl_4$] treatment. For permeabilization, cells were subsequently treated with 0.1% Triton X-100 and blocked with 1.5% bovine serum albumin (BSA) in PBS. Cells were then incubated with anti-αS primary antibody (BD 610787, 1:1000) and anti-V5 tag (Abcam ab9116, 1:100), either 4 h at room temperature or overnight at 4 °C, and 1 h in Alexa Fluor 488 donkey anti-rabbit and Alexa Fluor 555 donkey anti-mouse

as secondary antibodies (Invitrogen A21202 and A31570, respectively, 1:1000). Cells were further stained with Hoechst (Molecular Probes 33258) for 5–10 min. Images were captured using a Nikon C2 Plus confocal microscope.

Quantification of αS intracellular inclusions

Transfected cells were detected and scored based on the absence and presence of αS intracellular inclusions. We also quantify the pattern of αS intracellular inclusions, by classifying them in different groups: 1–4 inclusions, 5–9 inclusions and equal to/more than 10 inclusions. Results were expressed as the percentage of the total number of transfected cells obtained from three independent experiments [15]. At least 50–100 cells were counted per condition.

Results and discussion

Influence of metal coordination and peripheral substituents on the interaction of tetrapyrroles with αS

We investigated the details of the binding of [$Na_4(H_2PcTS)$] (Fig. 1b), its Zn-loaded form [$Zn(H_4PcTS)$] (Fig. 1c) and the [$H_2PrTPCl_4$] (Fig. 1d) to the protein αS by NMR spectroscopy. To analyze these interactions we used ^1H–^{15}N HSQC spectroscopy. The ^1H–^{15}N HSQC spectrum of a 100 μM sample of uniformly ^{15}N-labeled αS recorded in buffer A at 15 °C is shown in Fig. 2a. The resonances were well resolved, with a limited dispersion of chemical shifts, reflecting the disordered state and the high degree of flexibility of the backbone. As previously reported, the interaction of αS with [$Na_4(H_2PcTS)$] caused significant broadening and chemical shift changes in a number of residues at the N-terminal region of the protein [35] (Fig. 2b). No perturbations were observed for the amide groups of residues located in the NAC region or at the C terminus. Close analysis of the signals exhibiting severe changes on αS upon addition of [$Na_4(H_2PcTS)$] shows that the interaction is centered at Phe-4 and Tyr-39 residues. A small broadening and shift perturbation become also evident at Phe-94. The perturbations caused by the [$Zn(H_4PcTS)$] were also located at the N-terminal region of αS; however, the most affected residue was the histidine at position 50 (Fig. 2c). Minor effects were also detected at Phe-4 and Tyr-39, together with a lack of binding to Phe-94 (Fig. 2c). On the other hand, no broadening or chemical shift perturbations were detected when the interaction of αS with [$Al(H_4PcTS)Cl$] (Fig. S1) [37].

To evaluate the influence that charged substituents located at the periphery of the macrocycle might exert on the molecular interactions of these compounds with target proteins, we studied the binding features of the [$H_2PrTPCl_4$] molecule to the protein αS. Contrasting with the studied phthalocyanines, the substituents groups located at the periphery of the macrocycle in [$H_2PrTPCl_4$] are positively charged (*N*-methyl-4-pyridyl). As observed in Fig. 2d, the titration of αS with [$H_2PrTPCl_4$] caused broadening and chemical shift changes of amide resonances in the segment Q120–A140, located at the highly acidic C-terminal region of the protein. The residues exhibiting the strongest perturbations in the amide resonances were Tyr-125, Tyr-133 and Tyr-136 (Figs. 2d and S2). Thus, the substitution of the negatively charged sulfonate groups at peripheral positions of cyclic tetrapyrroles by positively charged *N*-methyl-pyridyl groups influences markedly the binding features of these molecules, by redirecting the interaction from the N-terminal region to the C-terminus of αS.

The interaction of the tetrapyrrolic compounds with aromatic moieties in the protein was then analyzed by NMR experiments aimed at detecting directly the selective perturbation of resonances of aromatic side chains in αS upon ligand binding (Fig. S3). The distribution of aromatic residues throughout the αS sequence provides excellent probes to investigate the interaction of cyclic tetrapyrroles with αS. The binding features observed for the [$Na_4(H_2PcTS)$], [$Zn(H_4PcTS)$] and [$H_2PrTPCl_4$] complexes confirm the role as anchoring moieties played by the aromatic side chains of Phe-4, Tyr-39, and His-50 at the N-terminus and by Tyr-125, Tyr-133 and Tyr-136 at the C-terminal region of αS (Fig. S3). In particular, these spectra allowed us to conclude that Phe-4 and Tyr-39 are the main anchoring residues for [$Na_4(H_2PcTS)$] binding to the N-terminal region of αS, highlighting the role of specific π–π interactions between the aromatic ring system of these molecules and aromatic residues in the amyloidogenic proteins in the formation of the αS-[$Na_4(H_2PcTS)$] complex. Interestingly, in the case of [$Zn(H_4PcTS)$], whereas the divalent cation Zn(II) was shown to bind preferentially to the C-terminus of αS [66], electrostatic repulsions between the peripheral sulfonate groups in the ring system and the highly negatively charged C-terminal region disfavor the location of the [$Zn(H_4PcTS)$] complex at that region, redirecting its binding toward the N-terminal interface. In that region, the His-50 residue acts as the main anchoring residue for [$Zn(H_4PcTS)$] binding, indicating that the preferential affinity of the Zn(II) ion coordinated to the center of the phthalocyanine modulates the binding features of this compound by targeting other binding site in the αS protein. Although more work is needed to confirm this hypothesis, this interpretation is in agreement with the more pronounced propensity of Zn(II) ions to form flexible and open coordination geometries, as we demonstrated recently for the interaction of [$Zn(H_4PcTS)$] with the amyloid β-peptide [36].

Clearly, the presence of positively charged substituents at the periphery of the macrocycle in the [$H_2PrTPCl_4$]

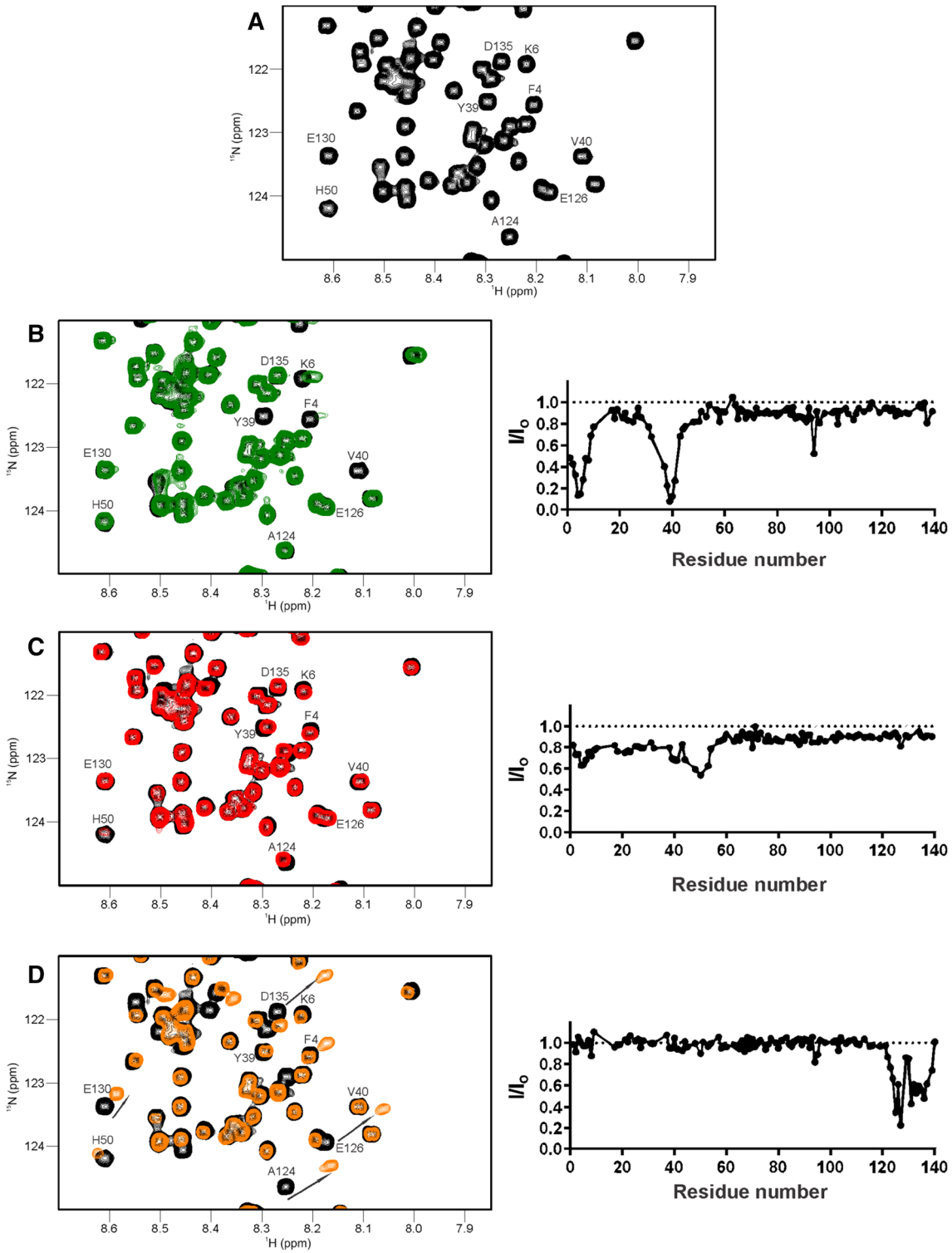

Fig. 2 Structural characterization of the interaction between phthalocyanines and [H_2PrTPCl$_4$] with αS monitored by NMR spectroscopy. **a** ^{1}H–^{15}N HSQC spectra of 100 μM αS. **b** Overlaid contour plots of ^{1}H–^{15}N HSQC spectra and I/I$_0$ profile of the backbone amide groups of 100 μM αS in the absence (black) or presence (green) of 50 μM [Na4(H_2PcTS)]. **c** Overlaid contour plots of ^{1}H–^{15}N HSQC spectra and *I*/*I*$_0$ profile of the backbone amide groups of 100 μM αS in the absence (black) or presence (red) of 50 μM [Zn(H_4PcTS)]. **d** Overlaid contour plots of ^{1}H–^{15}N HSQC spectra and *I*/*I*$_0$ profile of the backbone amide groups of 100 μM αS in the absence (black) and presence (orange) of 50 μM [H_2PrTPCl$_4$]. Amino acid residues of αS affected by the interaction with the tetrapyrrole compounds are identified. ^{1}H–^{15}N HSQC spectra were recorded at 15 °C using ^{15}N isotopically enriched αS (100 μM) samples

molecule allows this molecule to interact electrostatically with negative patches at the C-terminal region of αS, directing the location of the [H_2PrTPCl_4] molecule to that region of the protein structure. There, the cluster of tyrosines (Y-125, Y-133 and Y-136) at the C-terminus constitute the target site for [H_2PrTPCl_4] binding to αS, as shown in Figs. 2D and S2. As observed with the [Na_4(H_2PcTS)] molecule at the N-terminus binding interface, aromatic interactions between the macrocycle ring of [H_2PrTPCl_4] and the Tyr cluster at the C-terminus contribute strongly to the binding process.

Finally, from the analysis of panels b–d of Fig. 2 we also found indications of significant differences in the degree of broadening induced by [Na_4(H_2PcTS)], its Zn(II)-loaded form and [H_2PrTPCl_4] on the amide resonances of αS. We demonstrated previously that the degree of phthtalocyanines self-association corrrelates well with their capabilities to bind αS, with low order stacked aggregates of the cyclic tetrapyrroles being identified as the active interacting species [37]. The planarity and aromaticity of the central heterocycle appear to be determining factors for such self-association reactions, which, however, can be perturbed or heavily impaired by the nature of the conjugated metal ion. Indeed, the smaller effects induced by [Zn(H_4PcTS)] binding to αS reflect the lower tendency of this phthalocyanine derivative to self-associate [37]. As expected, this behavior becomes more evident in the Al(III) derivative, which was shown to remain mostly as a monomer in solution and thus, showed a complete lack of interaction with the protein (Fig. S1) [37]. In this compound, axial coordination of Al(III) with chloride anions give rises to distorted structures that impair the stacking of the [Al(H_4PcTS)Cl] molecules.

Effects of tetrapyrrolic compounds on the aggregation of αS in vitro and in cell-based model

Ultrastructural visualization of the final product of aggregation of αS using TEM shows that normal amyloid fibrils are formed in the absence of tetrapyrrolic compounds (Fig. 3a). We found that [Na_4(H_2PcTS)] and [Zn(H_4PcTS)] produced a variety of small, amorphous, non-fibrillar aggregates (Fig. 3b), as well as short, flat fibrillar αS aggregates, respectively (Fig. 3c). Conversely, the αS aggregates in [Al(H_4PcTS)Cl]-treated samples showed an amyloid morphology comparable with that of untreated protein samples (Figure S4). On the other hand, Fig. 3d shows that αS amyloid assembly through [H_2PrTPCl_4] mediation are made of large and abundant aggregates, comprising clusters of fibrils.

Finally, we tested the potential toxicity of phthalocyanines and [H_2PrTPCl_4] in human neuroglioma (H4) cells. For this cell line, the compounds were innocuous at concentrations as high as 20 μM (data not shown). Then, we used a well-established cell model to assess αS inclusion formation. H4 cells were transiently transfected with C-terminally modified αS (SynT) and synphilin-1, which results in the formation of LB-like inclusions, as previously described [15]. The formation of αS inclusions was assessed 48 h after treatment (Fig. 4a). Upon treatment with 10 μM [Na_4(H_2PcTS)] and [Zn(H_4PcTS)] we observed a significant increase in the number of transfected cells devoiding αS inclusions relative to untreated samples (Fig. 4b). Analysis of αS inclusion formation in the [Al(H_4PcTS)Cl]-treated cells showed a pattern comparable with that of untreated samples (Figs. 4a, b and S5). By contrast, [H_2PrTPCl_4] treatment promoted an increase in the number of transfected cells displaying αS aggregates (Figs. 4a, b and S5). Overall, our results

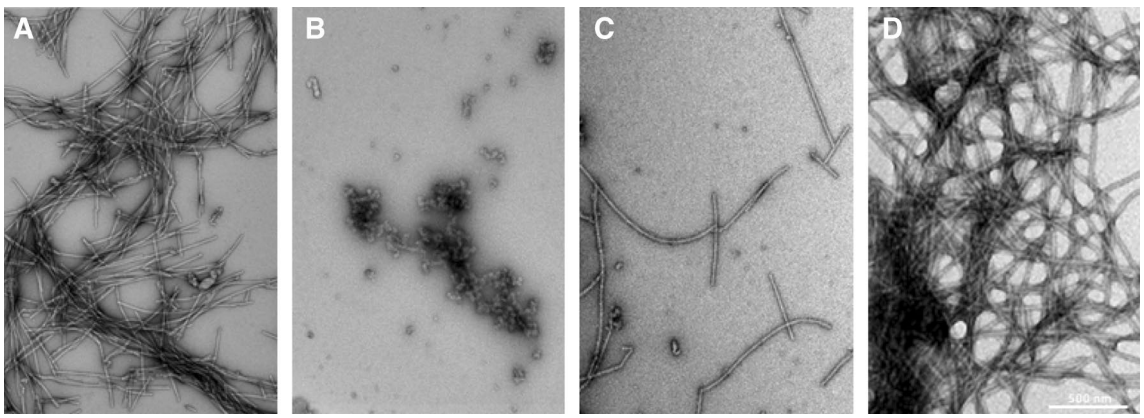

Fig. 3 Modulation of αS aggregation by phthalocyanines and [H_2PrTPCl_4]. Representative negative stain EM images of αS aggregates (100 μM samples) generated in **a** the absence and presence of 100 μM, **b** [Na4(H2PcTS)], **c** [Zn(H_4PcTS)] and **d** [H_2PrTPCl_4]. Fibrils of identical morphologies to that shown in panel A were obtained for αS in the presence of [Al(H_4PcTS)Cl] (Fig. S4)

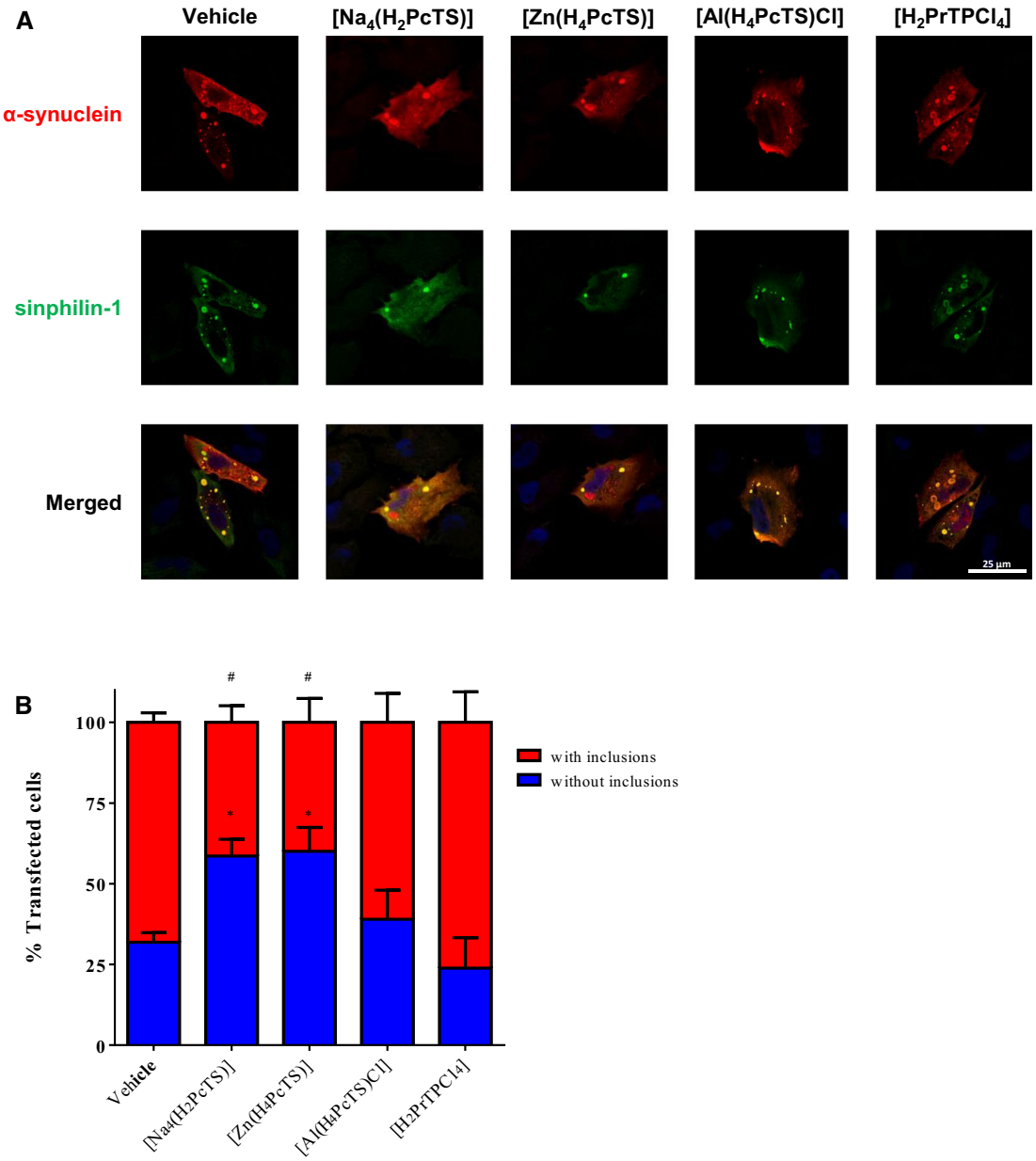

Fig. 4 Modulation of αS inclusion formation in cultured cells. **a** Representative images of intracellular αS inclusion formation in human cultured cells in the presence of phthalocyanines and [$H_2PrTPCl_4$]. Human H4 neuroglioma cells were co-transfected with plasmids encoding SynT and Synphilin-1, and inclusion formation was assessed 48 h post-transfection. Cells were incubated in the absence (vehicle) and the presence of the studied tetracyclic compounds (10 µM). **b** Quantification of αS inclusions. Transfected cells were detected and scored based on the absence or presence of αS inclusions. Results were expressed as the percentage of the total number of transfected cells obtained from three independent experiments. At least 50 cells were scored per experiment ($n=3$). A detailed quantification of the pattern of αS inclusion formation, in the absence or presence of the studied compounds is shown in Fig. S5. $^{*}p<0.05$ cells without inclusions vs. vehicle treatment; $^{\#}p<0.05$ cells with inclusions vs. vehicle treatment

demonstrated that the effects induced by phthalocyanines and [$H_2PrTPCl_4$] on αS fibril formation in vitro are reproduced well on the H4 cell-based model of αS aggregation.

Conclusions

The results reported in this work provide a firm basis to understand the structural rules directing the binding of tetrapyrrolic compounds to αS, and their implications for the amyloid aggregation of the protein. Because the structural basis for the activity of these molecules as modulators of

amyloid aggregation is starting to emerge, combined efforts from the fields of chemistry, structural and cell biology are needed at this stage to elucidate their binding modes with the target proteins, the precise molecular mechanism(s) of action of these molecules and its biological activity on cell models of the disease. The interaction scenario described in our work revealed that both N- and C-terminal regions of αS represent binding interfaces for the studied compounds, a behavior that is mainly driven by the presence of negatively or positively charged substituents located at the periphery of the macrocycle, that can mediate electrostatic interaction with positive or negative patches on the proteins structure. With the polyaromatic compounds located at the N- or C-terminus, the interaction mode is determined by (1) the planarity and hydrophobicity of the aromatic ring system in the tetrapyrrolic molecule and/or (2) the preferential affinity of the metal ion conjugated at the center of the macrocyclic ring.

The differences observed between the binding preferences and interaction profiles of [H_2PrTPCl$_4$] and phthalocyanines provide a structural explanation for the promotion of αS amyloid fibril formation by [H_2PrTPCl$_4$] molecules against the inhibitory effect exerted by [Na_4(H_2PcTS)]. Regarding to the mechanistic basis behind the inhibitory effects of [Na_4(H_2PcTS)] and [Zn(H_4PcTS)] on αS amyloid fibril assembly, the amyloid blocking effects of these phthalocyanines might be related to a loss of function of aromatic side chains involved in the filament-assembly mechanism, likely comprising early intra- and intermolecular interactions necessary for amyloid structural transition and implying to the affected residues. On the other hand, we propose that formation of the αS-[H_2PrTPCl$_4$] complex reduces and/or interferes with the attractive intramolecular interactions of the C-terminus with the N-terminal and NAC regions in the protein, decreasing the stability of monomeric αS and promoting its aggregation.

Interestingly, the different capability of phthalocyanines and [H_2PrTPCl$_4$] to modulate αS aggregation in vitro was also observed in cell-based models of PD, demonstrating unequivocally that the inhibitory mechanism exerted by phthalocyanines on amyloid assembly is a direct consequence of their interaction with target proteins. Added to that, the versatility of these compounds to condone the coordination of different metal ions and a wide range of peripheral substituents, which in turn can modulate physicochemical properties such as their solubility and distribution in biological fluids, emphasize the potential of this scaffold for further optimizations in terms of pharmacokinetics and delivery to the brain.

Acknowledgements C.O.F. thanks Universidad Nacional de Rosario (UNR) and ANPCyT- FONCyT (PICT 2014-3704 and PICT 2017-4665) for financial support. C.O.F. and C.G. thank the Max Planck Society (P10390) for support. C.O.F thanks Dietmar Riedel and Gudrum Heim for helpful assistance during the transmission electron microscopy measurements. N.G. and I.G. thanks UNR for fellowships. F.B. thanks CONICET for fellowship.

References

1. Gandhi S, Wood NW (2010) Genome-wide association studies: the key to unlocking neurodegeneration? Nat Neurosci 13:789–794. https://doi.org/10.1038/nn.2584
2. de Lau LML, Breteler MMB (2006) Epidemiology of Parkinson's disease. Lancet Neurol 5:525–535. https://doi.org/10.1016/S1474-4422(06)70471-9
3. Henchcliffe C, Beal MF (2008) Mitochondrial biology and oxidative stress in Parkinson disease pathogenesis. Nat Clin Pract Neurol 4:600–609. https://doi.org/10.1038/ncpneuro0924
4. Spillantini MG, Crowther RA, Jakes R et al (1998) Filamentous alpha-synuclein inclusions link multiple system atrophy with Parkinson's disease and dementia with Lewy bodies. Neurosci Lett 251:205–208. https://doi.org/10.1016/S0304-3940(98)00504-7
5. Papapetropoulos S, Adi N, Ellul J et al (2007) A prospective study of familial versus sporadic Parkinson's disease. Neurodegener Dis 4:424–427. https://doi.org/10.1159/000107702
6. Dawson TM, Dawson VL (2003) Rare genetic mutations shed light on the pathogenesis of Parkinson disease. J Clin Invest 111:145–151. https://doi.org/10.1172/JCI17575
7. McCann H, Stevens CH, Cartwright H, Halliday GM (2014) α-Synucleinopathy phenotypes. Parkinsonism Relat Disord 20(Suppl 1):S62–S67. https://doi.org/10.1016/S1353-8020(13)70017-8
8. Spillantini MG, Crowther RA, Jakes R et al (1998) alpha-Synuclein in filamentous inclusions of Lewy bodies from Parkinson's disease and dementia with lewy bodies. Proc Natl Acad Sci USA 95:6469–6473. https://doi.org/10.1073/pnas.95.11.6469
9. Volles MJ, Lansbury PT (2003) Zeroing in on the pathogenic form of alpha-synuclein and its mechanism of neurotoxicity in Parkinson's disease. Biochemistry 42:7871–7878. https://doi.org/10.1021/bi030086j
10. Cookson MR, van der Brug M (2008) Cell systems and the toxic mechanism(s) of alpha-synuclein. Exp Neurol 209:5–11. https://doi.org/10.1016/j.expneurol.2007.05.022
11. Eisbach SE, Outeiro TF (2013) Alpha-synuclein and intracellular trafficking: impact on the spreading of Parkinson's disease pathology. J Mol Med 91:693–703. https://doi.org/10.1007/s00109-013-1038-9
12. Roberts HL, Brown DR (2015) Seeking a mechanism for the toxicity of oligomeric α-synuclein. Biomolecules 5:282–305. https://doi.org/10.3390/biom5020282
13. Winner B, Jappelli R, Maji SK et al (2011) In vivo demonstration that alpha-synuclein oligomers are toxic. Proc Natl Acad Sci USA 108:4194–4199. https://doi.org/10.1073/pnas.1100976108
14. Karpinar DP, Balija MBG, Kügler S et al (2009) Pre-fibrillar alpha-synuclein variants with impaired beta-structure increase neurotoxicity in Parkinson's disease models. EMBO J 28:3256–3268. https://doi.org/10.1038/emboj.2009.257
15. Lázaro DF, Rodrigues EF, Langohr R et al (2014) Systematic comparison of the effects of alpha-synuclein mutations on its oligomerization and aggregation. PLoS Genet 10:e1004741. https://doi.org/10.1371/journal.pgen.1004741
16. Pokrzywa M, Pawełek K, Kucia WE et al (2017) Effects of small-molecule amyloid modulators on a Drosophila model of Parkinson's disease. PLoS One 12:e0184117. https://doi.org/10.1371/journal.pone.0184117

17. Kurnik M, Sahin C, Andersen CB et al (2018) Potent α-synuclein aggregation inhibitors, identified by high-throughput screening, mainly target the monomeric state. Cell Chem Biol 25:1389–1402. e9. https://doi.org/10.1016/j.chembiol.2018.08.005
18. Tonda-Turo C, Herva M, Chiono V et al (2018) Influence of drug-carrier polymers on alpha-synucleinopathies: a neglected aspect in new therapies development. Biomed Res Int 2018:4518060. https://doi.org/10.1155/2018/4518060
19. Trigo-Damas I, Del Rey NL-G, Blesa J (2018) Novel models for Parkinson's disease and their impact on future drug discovery. Expert Opin Drug Discov 13:229–239. https://doi.org/10.1080/17460441.2018.1428556
20. Maroteaux L, Campanelli JT, Scheller RH (1988) Synuclein: a neuron-specific protein localized to the nucleus and presynaptic nerve terminal. J Neurosci 8:2804–2815
21. Burré J, Sharma M, Südhof TC (2014) α-Synuclein assembles into higher-order multimers upon membrane binding to promote SNARE complex formation. Proc Natl Acad Sci USA 111:E4274–E4283. https://doi.org/10.1073/pnas.1416598111
22. Stefanis L (2012) α-Synuclein in Parkinson's disease. Cold Spring Harb Perspect Med 2:a009399. https://doi.org/10.1101/cshperspect.a009399
23. Sidhu A, Wersinger C, Vernier P (2004) Does alpha-synuclein modulate dopaminergic synaptic content and tone at the synapse? FASEB J 18:637–647. https://doi.org/10.1096/fj.03-1112rev
24. Yavich L, Tanila H, Vepsäläinen S, Jäkälä P (2004) Role of alpha-synuclein in presynaptic dopamine recruitment. J Neurosci 24:11165–11170. https://doi.org/10.1523/JNEUROSCI.2559-04.2004
25. Breydo L, Wu JW, Uversky VN (2012) A-synuclein misfolding and Parkinson's disease. Biochim Biophys Acta 1822:261–285. https://doi.org/10.1016/j.bbadis.2011.10.002
26. Dedmon MM, Lindorff-Larsen K, Christodoulou J et al (2005) Mapping long-range interactions in alpha-synuclein using spin-label NMR and ensemble molecular dynamics simulations. J Am Chem Soc 127:476–477. https://doi.org/10.1021/ja044834j
27. Bertoncini CW, Jung Y-S, Fernandez CO et al (2005) Release of long-range tertiary interactions potentiates aggregation of natively unstructured alpha-synuclein. Proc Natl Acad Sci USA 102:1430–1435. https://doi.org/10.1073/pnas.0407146102
28. Cho M-K, Nodet G, Kim H-Y et al (2009) Structural characterization of alpha-synuclein in an aggregation prone state. Protein Sci 18:1840–1846. https://doi.org/10.1002/pro.194
29. Chiti F, Dobson CM (2017) Protein misfolding, amyloid formation, and human disease: a summary of progress over the last decade. Annu Rev Biochem 86:27–68. https://doi.org/10.1146/annurev-biochem-061516-045115
30. Moriarty GM, Janowska MK, Kang L, Baum J (2013) Exploring the accessible conformations of N-terminal acetylated α-synuclein. FEBS Lett 587:1128–1138. https://doi.org/10.1016/j.febslet.2013.02.049
31. Kang L, Moriarty GM, Woods LA et al (2012) N-terminal acetylation of α-synuclein induces increased transient helical propensity and decreased aggregation rates in the intrinsically disordered monomer. Protein Sci 21:911–917. https://doi.org/10.1002/pro.2088
32. Liu T, Bitan G (2012) Modulating self-assembly of amyloidogenic proteins as a therapeutic approach for neurodegenerative diseases: strategies and mechanisms. ChemMedChem 7:359–374. https://doi.org/10.1002/cmdc.201100585
33. Villemagne VL, Doré V, Bourgeat P et al (2017) Aβ-amyloid and Tau Imaging in Dementia. Semin Nucl Med 47:75–88. https://doi.org/10.1053/j.semnuclmed.2016.09.006
34. Arja K, Sjölander D, Åslund A et al (2013) Enhanced fluorescent assignment of protein aggregates by an oligothiophene-porphyrin-based amyloid ligand. Macromol Rapid Commun 34:723–730. https://doi.org/10.1002/marc.201200817
35. Lamberto GR, Binolfi A, Orcellet ML et al (2009) Structural and mechanistic basis behind the inhibitory interaction of PcTS on alpha-synuclein amyloid fibril formation. Proc Natl Acad Sci USA 106:21057–21062. https://doi.org/10.1073/pnas.0902603106
36. Valiente-Gabioud AA, Riedel D, Outeiro TF et al (2018) Binding modes of phthalocyanines to amyloid β peptide and their effects on amyloid fibril formation. Biophys J 114:1036–1045. https://doi.org/10.1016/j.bpj.2018.01.003
37. Lamberto GR, Torres-Monserrat V, Bertoncini CW et al (2011) Toward the discovery of effective polycyclic inhibitors of alpha-synuclein amyloid assembly. J Biol Chem 286:32036–32044. https://doi.org/10.1074/jbc.M111.242958
38. Bulic B, Pickhardt M, Khlistunova I et al (2007) Rhodanine-based tau aggregation inhibitors in cell models of tauopathy. Angew Chem Int Ed Engl 46:9215–9219. https://doi.org/10.1002/anie.200704051
39. Schenk D, Basi GS, Pangalos MN (2012) Treatment strategies targeting amyloid β-protein. Cold Spring Harb Perspect Med 2:a006387. https://doi.org/10.1101/cshperspect.a006387
40. Masuda M, Suzuki N, Taniguchi S et al (2006) Small molecule inhibitors of alpha-synuclein filament assembly. Biochemistry 45:6085–6094. https://doi.org/10.1021/bi0600749
41. Caughey B, Caughey WS, Kocisko DA et al (2006) Prions and transmissible spongiform encephalopathy (TSE) chemotherapeutics: a common mechanism for anti-TSE compounds? Acc Chem Res 39:646–653. https://doi.org/10.1021/ar050068p
42. Ehrnhoefer DE, Bieschke J, Boeddrich A et al (2008) EGCG redirects amyloidogenic polypeptides into unstructured, off-pathway oligomers. Nat Struct Mol Biol 15:558–566. https://doi.org/10.1038/nsmb.1437
43. Caughey WS, Priola SA, Kocisko DA et al (2007) Cyclic tetrapyrrole sulfonation, metals, and oligomerization in antiprion activity. Antimicrob Agents Chemother 51:3887–3894. https://doi.org/10.1128/AAC.01599-06
44. Wagner J, Ryazanov S, Leonov A et al (2013) Anle138b: a novel oligomer modulator for disease-modifying therapy of neurodegenerative diseases such as prion and Parkinson's disease. Acta Neuropathol 125:795–813. https://doi.org/10.1007/s00401-013-1114-9
45. Levin J, Schmidt F, Boehm C et al (2014) The oligomer modulator anle138b inhibits disease progression in a Parkinson mouse model even with treatment started after disease onset. Acta Neuropathol 127:779–780. https://doi.org/10.1007/s00401-014-1265-3
46. Scherzer-Attali R, Shaltiel-Karyo R, Adalist YH et al (2012) Generic inhibition of amyloidogenic proteins by two naphthoquinone-tryptophan hybrid molecules. Proteins 80:1962–1973. https://doi.org/10.1002/prot.24080
47. Frydman-Marom A, Shaltiel-Karyo R, Moshe S, Gazit E (2011) The generic amyloid formation inhibition effect of a designed small aromatic β-breaking peptide. Amyloid 18:119–127. https://doi.org/10.3109/13506129.2011.582902
48. Frydman-Marom A, Rechter M, Shefler I et al (2009) Cognitive-performance recovery of Alzheimer's disease model mice by modulation of early soluble amyloidal assemblies. Angew Chem Int Ed Engl 48:1981–1986. https://doi.org/10.1002/anie.200802123
49. González-Lizárraga F, Socías SB, Ávila CL et al (2017) Repurposing doxycycline for synucleinopathies: remodelling of α-synuclein oligomers towards non-toxic parallel beta-sheet structured species. Sci Rep 7:41755. https://doi.org/10.1038/srep41755
50. Pujols J, Peña-Díaz S, Lázaro DF et al (2018) Small molecule inhibits α-synuclein aggregation, disrupts amyloid fibrils, and prevents degeneration of dopaminergic neurons. Proc Natl Acad

Sci USA 115:10481–10486. https://doi.org/10.1073/pnas.1804198115
51. Valdinocci D, Grant GD, Dickson TC, Pountney DL (2018) Epothilone D inhibits microglia-mediated spread of alpha-synuclein aggregates. Mol Cell Neurosci 89:80–94. https://doi.org/10.1016/j.mcn.2018.04.006
52. Schwab K, Frahm S, Horsley D et al (2017) A protein aggregation inhibitor, leuco-methylthioninium bis(hydromethanesulfonate), decreases α-synuclein inclusions in a transgenic mouse model of synucleinopathy. Front Mol Neurosci 10:447. https://doi.org/10.3389/fnmol.2017.00447
53. Palazzi L, Bruzzone E, Bisello G et al (2018) Oleuropein aglycone stabilizes the monomeric α-synuclein and favours the growth of non-toxic aggregates. Sci Rep 8:8337. https://doi.org/10.1038/s41598-018-26645-5
54. Jha NN, Kumar R, Panigrahi R et al (2017) Comparison of α-synuclein fibril inhibition by four different amyloid inhibitors. ACS Chem Neurosci 8:2722–2733. https://doi.org/10.1021/acschemneuro.7b00261
55. Reiner AM, Schmidt F, Ryazanov S et al (2018) Photophysics of diphenyl-pyrazole compounds in solutions and α-synuclein aggregates. Biochim Biophys Acta Gen Subj 1862:800–807. https://doi.org/10.1016/j.bbagen.2017.12.007
56. Valiente-Gabioud AA, Miotto MC, Chesta ME et al (2016) Phthalocyanines as molecular scaffolds to block disease-associated protein aggregation. Acc Chem Res 49:801–808. https://doi.org/10.1021/acs.accounts.5b00507
57. Fonseca-Ornelas L, Eisbach SE, Paulat M et al (2014) Small molecule-mediated stabilization of vesicle-associated helical α-synuclein inhibits pathogenic misfolding and aggregation. Nat Commun 5:5857. https://doi.org/10.1038/ncomms6857
58. Akoury E, Gajda M, Pickhardt M et al (2013) Inhibition of tau filament formation by conformational modulation. J Am Chem Soc 135:2853–2862. https://doi.org/10.1021/ja312471h
59. Chakraborty R, Sahoo S, Halder N et al (2019) Conformational-switch based strategy triggered by [18] π heteroannulenes toward reduction of alpha synuclein oligomer toxicity. ACS Chem Neurosci 10:573–587. https://doi.org/10.1021/acschemneuro.8b00436
60. Caughey B, Lansbury PT (2003) Protofibrils, pores, fibrils, and neurodegeneration: separating the responsible protein aggregates from the innocent bystanders. Annu Rev Neurosci 26:267–298. https://doi.org/10.1146/annurev.neuro.26.010302.081142
61. Caughey WS, Raymond LD, Horiuchi M, Caughey B (1998) Inhibition of protease-resistant prion protein formation by porphyrins and phthalocyanines. Proc Natl Acad Sci USA 95:12117–12122. https://doi.org/10.1073/pnas.95.21.12117
62. Priola SA, Raines A, Caughey WS (2000) Porphyrin and phthalocyanine antiscrapie compounds. Science 287:1503–1506
63. Johnson M, Geeves MA, Mulvihill DP (2013) Production of amino-terminally acetylated recombinant proteins in *E. coli*. Methods Mol Biol 981:193–200. https://doi.org/10.1007/978-1-62703-305-3_15
64. Hoyer W, Cherny D, Subramaniam V, Jovin TM (2004) Impact of the acidic C-terminal region comprising amino acids 109-140 on alpha-synuclein aggregation in vitro. Biochemistry 43:16233–16242. https://doi.org/10.1021/bi048453u
65. Cavanagh J, Fairbrother W, Palmer A III, Skelton N (1995) Protein NMR spectroscopy: principles and practice. Academic Press. ISBN: 9780080515298
66. Valiente-Gabioud AA, Torres-Monserrat V, Molina-Rubino L et al (2012) Structural basis behind the interaction of Zn^{2+} with the protein α-synuclein and the Aβ peptide: a comparative analysis. J Inorg Biochem 117:334–341. https://doi.org/10.1016/j.jinorgbio.2012.06.011